online data

Critical roles for p22^{phox} in the structural maturation and subcellular targeting of Nox3

Yoko NAKANO*†, Botond BANFI*‡, Algirdas J. JESAITIS§, Mary C. DINAUER‖, Lee-Ann H. ALLEN*† and William M. NAUSEEF*†[1]

*Inflammation Program, University of Iowa and Veterans Affairs Medical Center, Iowa City, IA 52241, U.S.A., †Department of Medicine, University of Iowa and Veterans Affairs Medical Center, Iowa City, IA 52241, U.S.A., ‡Department of Anatomy and Cell Biology, University of Iowa and Veterans Affairs Medical Center, Iowa City, IA 52241, U.S.A., §Department of Microbiology, Montana State University, Bozeman, MT 59717, U.S.A., and ‖Wells Center for Pediatric Research, Department of Pediatrics (Hematology/Oncology), Microbiology/Immunology, and Medical and Molecular Genetics, Indiana University School of Medicine, Indianapolis, IN 46202, U.S.A.

Otoconia are small biominerals in the inner ear that are indispensable for the normal perception of gravity and motion. Normal otoconia biogenesis requires Nox3, a Nox (NADPH oxidase) highly expressed in the vestibular system. In HEK-293 cells (human embryonic kidney cells) transfected with the Nox regulatory subunits NoxO1 (Nox organizer 1) and NoxA1 (Nox activator 1), functional murine Nox3 was expressed in the plasma membrane and exhibited a haem spectrum identical with that of Nox2, the electron transferase of the phagocyte Nox. *In vitro* Nox3 cDNA expressed an ~50 kDa primary translation product that underwent N-linked glycosylation in the presence of canine microsomes. RNAi (RNA interference)-mediated reduction of endogenous p22^{phox}, a subunit essential for stabilization of Nox2 in phagocytes, decreased Nox3 activity in reconstituted HEK-293 cells. p22^{phox} co-precipitated not only with Nox3 and NoxO1 from transfectants expressing all three proteins, but also with NoxO1 in the absence of Nox3, indicating that p22^{phox} physically associated with both Nox3 and with NoxO1. The plasma membrane localization of Nox3 but not of NoxO1 required p22^{phox}. Moreover, the glycosylation and maturation of Nox3 required p22^{phox} expression, suggesting that p22^{phox} was required for the proper biosynthesis and function of Nox3. Taken together, these studies demonstrate critical roles for p22^{phox} at several distinct points in the maturation and assembly of a functionally competent Nox3 in the plasma membrane.

Key words: flavocytochrome b_{558}, glycosylation, haem spectrum, NADPH oxidase 3 (Nox3), Nox organizer 1 (NOXO1), p22^{phox}.

INTRODUCTION

The essential contribution of the phagocyte Nox (NADPH oxidase) to the antimicrobial activity of human neutrophils is widely recognized [1–3]. The multicomponent Nox responsible for oxidant production by stimulated neutrophils includes the integral membrane protein flavocytochrome b_{558}, which is a heterodimer composed of gp91^{phox} and p22^{phox} [4,5]. Neutrophils that lack normal gp91^{phox} or p22^{phox} fail to generate reactive oxygen species when stimulated, resulting in chronic granulomatous disease, a clinical disorder associated with frequent and severe infection [6]. As the electron transferase in flavocytochrome b_{558}, gp91^{phox} shuttles electrons donated by cytosolic NADPH across a pair of haem groups stacked within the membrane to reduce molecular oxygen and thereby generate superoxide anion. Although extensively studied by a variety of immunochemical and analytical techniques, the physical structure of flavocytochrome b_{558} has not been solved.

Given the importance of the phagocyte Nox in normal host defence [7], many of the biochemical features of its assembly as well as features of the structure, function and biosynthesis of flavocytochrome b_{558} have been the object of extensive study [4,5,8–10]. In cultured human promyelocytic cell lines, heterodimer formation in the ER (endoplasmic reticulum) is an essential step in biosynthesis required for subsequent plasma membrane targeting of flavocytochrome b_{558} [8–10]. Whereas nascent heterodimers acquire haem in the ER and subsequently undergo post-translational modification of N-linked oligosaccharides in the Golgi *en route* to the plasma membrane [10], free p22^{phox} or free gp91^{phox} lacks haem and undergoes ER-associated degradation [10]. Therefore the association of p22^{phox} with the biosynthetic precursor of gp91^{phox} in the ER is an early prerequisite for the expression of functional flavocytochrome b_{558} at the cell surface.

Based on sequence similarities, homologues of gp91^{phox} have been identified and collectively recognized as the Nox protein family, with gp91^{phox} designated as Nox2 [11]. Like gp91^{phox}, Nox3 requires protein cofactors for activity, as Nox3 alone does not support constitutive superoxide production in transfected cell lines [12]. In the presence of NoxO1 (Nox organizer 1) and NoxA1 (Nox activator 1), the homologues of p47^{phox} and p67^{phox} respectively in the phagocyte Nox [13,14], murine Nox3 supports robust constitutive superoxide production [12]. Of interest, and currently unexplained, human Nox3 is NoxA1-independent [13,15,16]. Although significant progress has been made in elucidating the tissue distribution and physiological functions of the newly recognized Nox protein family members, little is known about their biosynthesis or structural features beyond what can be predicted from cDNA sequence data.

In the present study, we focus on Nox3, the closest homologue of gp91^{phox} (58 % identity) in the Nox protein family [11]. Expressed in the inner ear of mice, Nox3 probably functions in normal biosynthesis or crystallization of otoconia, as mutations in Nox3 [17] or in the regulatory subunit NoxO1 [16] result in severe vestibular dysfunction. In the absence of primary cells or transformed cell lines that express endogenous Nox3, we used HEK-293 cells (human embryonic kidney cells) and CHO (Chinese

Abbreviations used: CHO, Chinese-hamster ovary; DTT, dithiothreitol; ER, endoplasmic reticulum; GFP, green fluorescent protein; EGFP, enhanced GFP; HEK-293 cells, human embryonic kidney cells; Nox, NADPH oxidase; NoxA1, Nox activator 1; NoxO1, Nox organizer 1; NP40, Nonidet P40; PNGase F, peptide:N-glycosidase F; PX domain, Phox homology domain; RNAi, RNA interference; SA, succinylacetone (4,6-dioxoheptanoic acid); SH3, Src homology 3; siRNA, small interfering RNA; SOD, superoxide dismutase; TNT, transcription and translation; WGA, wheat germ agglutinin.

[1] To whom correspondence should be addressed, at Inflammation Program, Department of Medicine, University of Iowa, D160 MTF, 2501 Crosspark Road, Coralville, IA 52241, U.S.A. (email william-nauseef@uiowa.edu).

hamster ovary)-K1 cells to express Nox3 and its cofactors heterologously. We demonstrate that functional membrane-bound Nox3 has the same spectral properties as does flavocytochrome b_{558}, undergoes co-translational glycosylation and subsequent oligosaccharide maturation *en route* to the plasma membrane, and forms heterodimers with p22^{phox} that are essential for its optimal targeting at the cell surface.

EXPERIMENTAL

Material

[^{35}S]Methionine/cysteine (26.57×10^7 Bq/0.5 ml), Protein A–Sepharose CL-4B and Gamma Bind Protein G–Sepharose were obtained from Amersham Biosciences (Piscataway, NJ, U.S.A.). A rabbit reticulocyte lysate kit for TNT (transcription and translation) reactions was purchased from Promega (Madison, WI, U.S.A.). PNGase F (peptide:N-glycosidase F) from *Chryseobacterium meningosepticum* was obtained from Calbiochem (La Jolla, CA, U.S.A.). Polyclonal rabbit anti-p22^{phox} antibody (FL-195) was from Santa Cruz Biotechnology (Santa Cruz, CA, U.S.A.). Monoclonal anti-GFP (green fluorescent protein) antibody (3E6, mouse IgG2a), anti-GFP rabbit serum, monoclonal anti-porin (human mitochondrial) antibody (31HL, mouse IgG2b) and monoclonal anti-cytochrome oxidase subunit IV (10G8, mouse IgG2a) were purchased from Molecular Probes Invitrogen Detection Technologies (Eugene, OR, U.S.A.). Monoclonal antibody JLA20 against actin was obtained from Calbiochem. Polyclonal rabbit anti-DsRed antibody and pDsRed-Monomer-C1 vector were obtained from BD Biosciences Clontech (Palo Alto, CA, U.S.A.). Monoclonal anti-p22^{phox} antibodies, CS9 (mouse IgG1) and 44.1 (mouse IgG2a), and monoclonal anti-gp91^{phox} antibody (54.1, mouse IgG1) were provided by Dr Algirdas Jesaitis.

Unless otherwise specified, all other reagents were purchased from Sigma–Aldrich (St. Louis, MO, U.S.A.).

Cell culture

HEK-293 cells were maintained in Dulbecco's modified Eagle's medium/Ham's nutrient mixture F12 containing 10 % (v/v) fetal calf serum, 100 units/ml penicillin, 100 μg/ml streptomycin, 100 mM Hepes and 2 mM L-glutamine. CHO-K1 cells were maintained in Ham's F12 medium containing 10 % fetal calf serum, 100 units/ml penicillin, 100 μg/ml streptomycin, 100 mM Hepes and 2 mM L-glutamine. For the generation of CHO cells stably transfected with p22^{phox} (p22^{phox}-CHO), cells were transfected with the human p22^{phox} cDNA in a pEF-PGKneo plasmid using Lipofectamine^{TM} 2000 (Invitrogen) as previously described [9]. Stably transfected clones were selected in a medium containing 1.8 mg/ml G418 and the expression of p22^{phox} was confirmed by immunoblotting. Tissue culture reagents for CHO cells and HEK-293 cells were obtained from Gibco (Invitrogen).

Subcloning and transfection

Human gp91^{phox} cDNA and p22^{phox} cDNA were cloned into pcDNA3.1 (Invitrogen, Carlsbad, CA, U.S.A.) and transfected to HEK-293 cells using the Effectene transfection system (Qiagen, Valencia, CA, U.S.A.). Stably transfected clones were selected in a medium containing 800 μg/ml G418 added 48 h after transfection. After 2 weeks, surviving clones were screened for expression of gp91^{phox} and p22^{phox} using flow cytometry and the anti-gp91^{phox} monoclonal antibody (7D5) [18–20] and by immunoblotting with anti-gp91^{phox} monoclonal antibody (54.1) [21] and anti-p22^{phox} monoclonal antibody (44.1) [22] respectively.

To generate cDNA encoding N-terminal DsRed-fusion protein of mouse Nox3, Nox3 cDNA was amplified using sense primer (5′-CTCGAGCTCCGGTGTGCTGGATTCTGAACGA-3′) and antisense primer (5′-CCGCGGCTAGAAGTTTTCCTTGTTG-TAATAGAA-3′). The PCR products containing XhoI and SacII sites were subcloned into the pDsRed-Monomer-C1 vector (BD Biosciences Clontech) and verified by DNA sequencing. Nox3, NoxO1, NoxA1-pcDNA3.1, NoxO1–EGFP (enhanced GFP) and Nox3–DsRed were transiently transfected into HEK-293 cells using the Effectene transfection system (Qiagen).

In vitro TNT

The cDNA for murine Nox3 and human gp91^{phox} were transcribed and translated *in vitro* using a rabbit reticulocyte lysate assay according to the manufacturer's instructions. Then, 5 μl of each reaction mixture was resolved by 5–20 % gradient SDS/PAGE. Gels were fixed, soaked in 1.2 M sodium salicylate, dried, and then exposed to a Kodak X-Omat film for 1–6 h at − 80 °C prior to autoradiography.

Spectroscopic examination of membranes

Wild-type or stably transfected HEK-293 cells were harvested from culture, washed in Hanks balanced salt solution three times, suspended in a buffer [20 mM Hepes, 0.25 M sucrose with 0.1 mM DTT (dithiothreitol), 1 mM PMSF, 10 μg/ml chymostatin and 1 μg/ml protease inhibitor cocktail (Sigma P-8340), pH 7.4], and disrupted using a glass Dounce homogenizer with a loose fitting pestle. The homogenate was first centrifuged at low speed (1000 ***g*** for 7 min at 4 °C) to remove nuclei and unbroken cells, and the resulting supernatant was centrifuged at 8000 ***g*** for 10 min at 4 °C to pellet mitochondria (P2). The supernatant (S2) was then centrifuged at 114000 ***g*** for 60 min at 4 °C to yield the plasma membrane-enriched pellet (P3). P2 and P3 were each suspended in solubilization buffer (100 mM KCl, 10 mM NaCl, 10 mM Hepes and 1 mM EDTA, pH 7.4, containing 0.1 mM DTT, 1 mM PMSF, 10 μg/ml chymostatin and 1 μg/ml protease inhibitor cocktail) and stored at –80 °C until use.

The isolated membrane pellets were washed in 1 M NaCl to remove associated cytosolic or peripheral membrane proteins [23] and centrifuged at 114000 ***g*** for 30 min at 4 °C. The washed membranes were resuspended in the homogenization buffer with sufficient 20 % (w/v) Triton X-100 to make the sample up to 1 % Triton X-100. The Triton X-100-solubilized membrane was sonicated on ice, using a Fisher Model 50 sonic dismembranator (Fisher Scientific, Pittsburgh, PA, U.S.A.; power setting no. 3), three times for 5 s each, and then incubated with stirring for 1 h at 4 °C. The solubilized membrane was centrifuged at 110000 ***g*** for 30 min at 4 °C to remove any debris before performing spectroscopy.

Spectroscopy was performed using a Lambda 40 spectrophotometer (PerkinElmer, Norwalk, CT, U.S.A.). The reduced-minus-oxidized spectra of the P2 and P3 from each of the membrane fractions (5×10^8 cells equivalent/ml) were measured, adding a few grains of sodium dithionite to the reduced sample. Flavocytochrome b_{558} or Nox3 was quantified from dithionite-reduced minus oxidized spectrum by measuring the absorbance difference between the peak at 558 nm and the trough at 540 nm and calculating the concentration using $\Delta\varepsilon_{558\text{-}540}$ 21.6 $mM^{-1} \cdot cm^{-1}$ (where ε is molar absorption coefficient) as previously described [24]. The value for membranes from untransfected HEK-293 cells was subtracted from the results to eliminate the contribution of the background and the results are expressed both as pmoles per 10^8 cells and per milligram of membrane protein. The P2 and P3 from each cell line were also separated by SDS/PAGE and

immunoblotted, probing with anti-cytochrome *c* and anti-porin antibodies to detect the presence of mitochondria.

Recovery of biosynthetically radiolabelled p22^{phox}

Wild-type or transfected HEK-293 cells were starved for 1 h in methionine-free medium supplemented with dialysed fetal calf serum and then radiolabelled with 59.2×10^4 Bq/ml [^{35}S]methionine for 1 h at 37 °C. Cells were recovered and solubilized in homogenate buffer as described above for membrane solubilization. The cell lysate (0.5–1.0 ml) was incubated with anti-p22^{phox} antibody (CS9) or isotype control IgG1 (10 μg/ml) at 4 °C with continuous rotation, and immune complexes were captured using Protein G–Sepharose. Washed beads were solubilized in SDS sample buffer, and proteins were resolved by SDS/PAGE and visualized by autoradiography as described above for the TNT reactions.

Detection of NoxO1–EGFP interactions with p22^{phox}

In the absence of antibodies that immunoprecipitate NoxO1, we created a NoxO1–EGFP construct to assess the interactions of NoxO1 with p22^{phox}. HEK-293 cells transfected with NoxO1–EGFP or vector control were solubilized, as described above, and then supplemented with 1 % deoxycholic acid, 1 % NP40 (Nonidet P40) and 0.05 % SDS. The solubilized cell lysate was incubated with purified monoclonal anti-GFP antibody or isotype control IgG2a at 4 °C. Immune complexes were captured using Protein A–Sepharose beads and then washed. Immunoprecipitations for p22^{phox} were performed as described above. Immune complexes were resolved by SDS/PAGE and immunoblots were probed with polyclonal antibodies against p22^{phox} or anti-GFP. Proteins were visualized with Enhanced Chemiluminescence reagents and a secondary antibody conjugated to horseradish peroxidase (SuperSignal substrate, Pierce, Rockford, IL, U.S.A.).

PNGase F digestion

Solubilized membrane fractions (9×10^7 cells) prepared as described above were denatured by heating in the presence of 0.1 % SDS and 1 % 2-mercaptoethanol. After cooling to room temperature, 10 μg/ml chymostatin, 1 μl/ml protease inhibitor, 1 mM PMSF and 10 mM EDTA were added to the denatured membrane solution followed by digestion using 5 units of PNGase F for 8 h at 37 °C.

RNAi (RNA interference)

The Stealth™ RNAi system (Invitrogen) was used to transiently knock down intracellular levels of p22^{phox}. The specific sequences for RNAi and for the scrambled control were: siRNA (small interfering RNA), sense 5′-GUGGUACUUUGGUGCCUACUCCAUU-3′ and antisense 5′-AAUGGAGUAGGCACCAAAGUACCAC-3′; scrambled control, sense 5′-GUGUUCAUGGUUCCGCUCACUGAUU-3′ and antisense 5′-AAUCAGUGAGCGGAACCAUGAACAC-3′. siRNA or scrambled control (100 pmol) was transfected into $0.5–1 \times 10^6$ Nox3 NoxO1A1-transfected HEK-293 cells using Lipofectamine™ 2000 transfection reagent (Invitrogen). Using the fluorescent oligonucleotide BLOCK-it™ Fluorescent Oligo (Invitrogen), the efficiency of transfection was determined to be > 80 %. Four days after treatment, the cells were collected for the experiment. The p22^{phox} protein levels were analysed by immunoblotting using a polyclonal antibody specific for p22^{phox}, and functional activity was assessed by measuring superoxide anion production, using the cytochrome *c* reduction assay as described below.

Superoxide anion measurement

Superoxide production was measured spectrophotometrically as the SOD (superoxide dismutase)-inhibitable reduction of ferricytochrome *c*, as described previously [25,26]. Briefly, washed wild-type cells or Nox3O1A1-transfected HEK-293 cells were incubated for 1 h at 37 °C in the presence of 80 μM ferricytochrome *c* without or with 200 units/ml of SOD. The amount of reduced ferricytochrome *c* was measured spectrophotometrically at 550 nm and the amount of superoxide generated was calculated using a molar absorption coefficient of 21.1 $mM^{-1} \cdot cm^{-1}$ at 550 nm and normalized to 10^6 cells.

SDS/PAGE and blotting

Proteins were separated by SDS/5–20 % PAGE and electroblotted on to nitrocellulose membranes. Membranes were blocked by incubation in PBS containing 5 % (w/v) non-fat milk, 0.1 % NP40 and 0.05 % sodium azide. The primary antibodies in dilution buffer [3 % (w/v) BSA, 0.1 % NP40 and 0.05 % sodium azide/PBS) at 1:1000 (anti-p22^{phox} antibody, 54.1, 44.1, GFP), 1:2000 (anti-cytochrome *c*, porin), 1:3000 (anti-actin) or 1:16 000 (anti-DsRed antibody) were added and the membrane was incubated overnight at 4 °C. The filter was washed (0.1 % BSA and 0.05 % Tween 20/PBS) and then incubated with horseradish peroxidase-conjugated secondary antibody diluted in washing buffer (0.1 % BSA and 0.05 % Tween 20/PBS) at 1:10 000 (anti-rabbit IgG or anti-mouse IgG). The filter was washed for 10 min seven times and proteins recognized by the specific antibody were visualized with the Enhanced Chemiluminescence detection system.

Confocal microscopy

The transfected cells were plated on glass coverslips 1 day before the samples were collected for analysis. Cells were washed in PBS and fixed in 10 % (v/v) formalin for 20 min at room temperature (20 °C). To examine the subcellular localization of NoxO1–EGFP and DsRed–Nox3, fixed cells were stained with Alexa Fluor® 594- or 488-conjugated WGA (wheat germ agglutinin; Invitrogen), to detect the plasma membrane and Golgi [27,28]. To examine the subcellular localization of p22^{phox}, the fixed cells were permeabilized in 0.2 % Triton X-100 for 2 min. Then, polyclonal rabbit anti-p22^{phox} antibody (FL-195) (Santa Cruz Biotechnology) and the Tyramine Signal Amplification kit (Invitrogen) were used for immunostaining according to the manufacturer's instructions. Images were obtained using LSM-510 confocal microscopy (Carl Zeiss, Thornwood, NY, U.S.A.).

RESULTS AND DISCUSSION

Spectroscopy of Nox3

gp91^{phox}, the prototypical member of the Nox protein family, is a *b*-type cytochrome and, partnered with p22^{phox} in the membrane, functions as the electron transferase of the phagocyte Nox [1]. Experimental data suggest that gp91^{phox} possesses two haem groups, each ligated to the protein backbone by histidine residues and oriented in a bis-haem motif common to several membrane cytochromes [29,30]. The histidines implicated by mutagenesis studies to ligate haem [30] are conserved in Nox3, suggesting that the same bis-haem organization may underlie the electron transferase activity of Nox3. In the absence of a cultured cell line that expresses endogenous Nox3, we utilized a heterologous expression system as a source of functional Nox3.

HEK-293 cells stably transfected with murine Nox3 and the essential cofactors NoxO1 and NoxA1 [12], homologues of

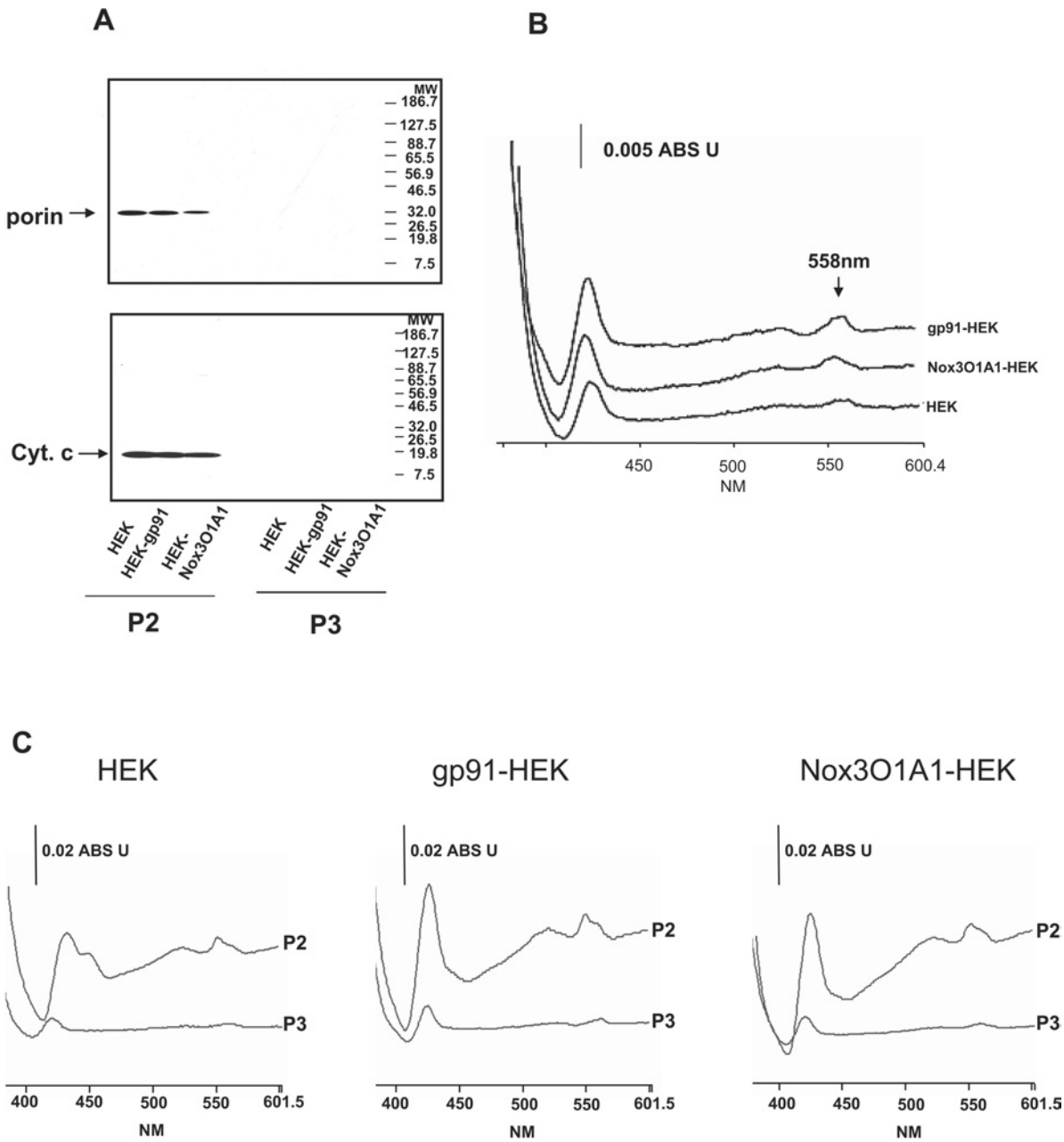

Figure 1 Haem spectrum of Nox3

(**A**) Membrane fractions enriched for mitochondria (P2) or plasma membrane (P3) from wild-type HEK-293 cells, HEK-293 transfectants expressing gp91^{phox}, or Nox3O1A1 were recovered by differential centrifugation, resolved by SDS/PAGE, and probed for the presence of the mitochondrial proteins cytochrome *c* and porin. Neither mitochondrial marker was detected in the P3 membrane. (**B**) Reduced-minus-oxidized spectra of the P3 from Nox3A1O1-transfected, gp91^{phox}-transfected or non-transfected HEK-293 cells (5×10^8 cells/ml) were measured as described in the Experimental section. Flavocytochrome *b* concentration was calculated using $\Delta\varepsilon_{588-540}$ 21.6 $mM^{-1} \cdot cm^{-1}$ as previously described [24]. The transfected cell lines had very similar amounts of haem protein in their membranes: 10.0 pmol/10^8 cells or 40.8 pmol/mg of protein for gp91^{phox} and 5.3 pmol/10^8 cells or 18.8 pmol/mg of protein for Nox3. (**C**) Reduced-minus-oxidized spectra of the P2 and P3 from Nox3A1O1-transfected, gp91^{phox}-transfected or non-transfected HEK-293 cells (5×10^8 cells/ml) were measured as in (**B**). The P3 spectra are the same as those in (**B**) but displayed on the same scale as optimally represents the P2 spectra. The broad peaks in the 540–560 nm range of P2 samples are essentially the same in all three cell types and distinctly different from the P3 peaks. NM, nm; ABS U, absorbance unit.

p47^{phox} and p67^{phox} respectively [13,14], constitutively generate significant amounts of superoxide anion extracellularly [12], indicating that Nox3 localizes in HEK-293 plasma membrane in the same orientation as gp91^{phox} in phagocytes. Concerned that the spectra of mitochondrial cytochromes contaminating membrane fractions derived from HEK-293 cells might obscure detection of the Nox3 spectrum in transfectants, we used differential centrifugation to recover subcellular fractions enriched for plasma membrane (P3) or mitochondria (P2). Based on immunoblotting of mitochondrial proteins porin and cytochrome oxidase subunit IV (Figure 1A), there was no detectable mitochondrial contamination of the P3 prepared from each of the HEK-293 cell lines and the mitochondrial proteins were restricted to P2. The dithionite-reduced minus oxidized spectra of P3 from gp91^{phox}–p22^{phox} transfectants (Figure 1B) demonstrated the expected peak at 558 nm characteristic of flavocytochrome b_{558} [24,31,32]. The washed P3

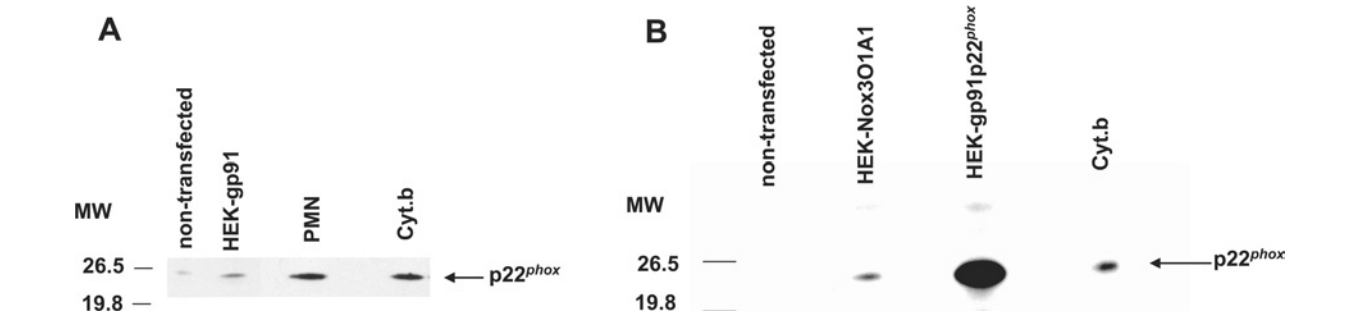

Figure 2 p22^{phox} protein in Nox-transfected cells

(**A**) Cell lysates (5×10^6 cell equivalents per lane) from untransfected wild-type HEK-293 cells or HEK-293 cells stably transfected with gp91^{phox} were immunoblotted with the murine monoclonal antibody 44.1. PMN membranes and purified flavocytochrome b_{558} were used as a positive control for p22^{phox}. Immunoblots were stripped and reprobed with actin antibody and signals quantified. Normalized for actin, gp91^{phox}-transfected cells expressed 3.90 ± 0.57-fold more p22^{phox} relative to that in wild-type HEK-293 cells ($n = 3$). Transfection of HEK-293 cells increased the steady-state level of p22^{phox}. (**B**) Cells lysates (5×10^7 cell equivalents per lane) from untransfected, Nox3O1A1-transfected, or gp91^{phox}/p22^{phox}-transfected HEK-293 cells were resolved by SDS/PAGE and probed for p22^{phox}. In comparison with levels of endogenous p22^{phox} in wild-type HEK-293 cells, the Nox3O1A1 transfectants had greater steady-state amounts of p22^{phox}. Purified flavocytochrome b_{558} was included as a standard for p22^{phox}. MW, molecular mass markers in kDa.

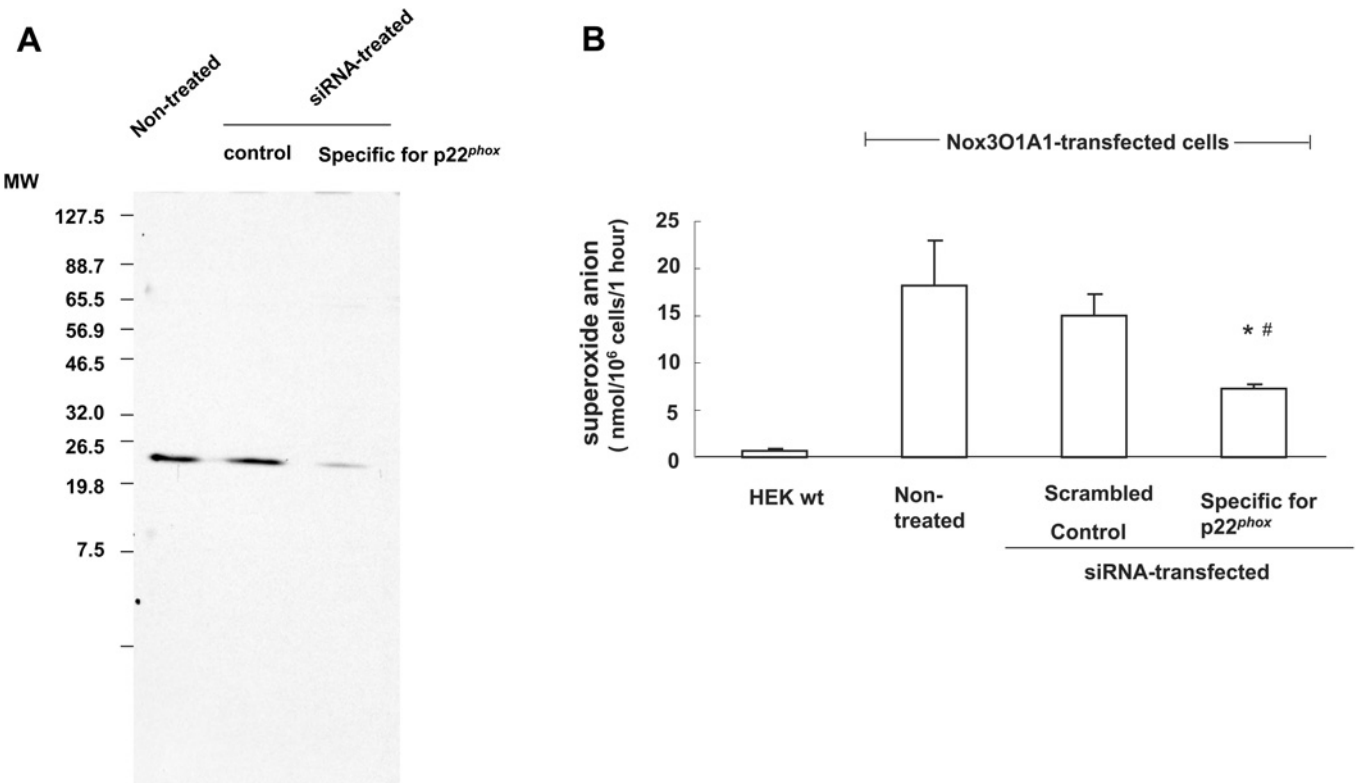

Figure 3 Knock-down of p22^{phox} decreased Nox3 activity

(**A**) siRNA specific for p22^{phox} or a scrambled siRNA (control) was introduced into Nox3O1A1-transfected HEK-293 cells. Four days after treatment, cells were solubilized, resolved by SDS/PAGE and probed for p22^{phox}. The specific siRNA decreased p22^{phox} levels to 12 % of the non-treated cells or of the cells treated with the scrambled RNA. (**B**) Cells treated with siRNA specific for p22^{phox} or scrambled RNA were assessed for superoxide production, using the ferricytochrome *c* assay. Constitutive superoxide production by Nox3O1A1 cells was reduced by p22^{phox}-specific siRNA. Values are means $\pm$ S.D. ($n = 4$). *$P < 0.05$, compared with untransfected cells. #$P < 0.05$, compared with scrambled control RNA. MW, molecular mass markers in kDa; wt, wild-type.

from Nox3O1A1 stable transfectants likewise exhibited a peak at 558 nm and, using the molar absorption coefficient of flavocytochrome b_{558} [24,31,32], expressed 18.8 pmol of Nox3/mg of membrane protein, less than half of that of Nox2 in the gp91^{phox} cells (40.8 pmol/mg of protein). As expected, the amount of overall cytochrome content in the mitochondria-rich P2 was much greater than the levels of Nox protein expressed in plasma membrane-rich P3, as demonstrated spectroscopically by a 25-fold shift in the absorbance scale (Figure 1C). Furthermore, the P2 samples from each cell line had nearly identical spectra with a peak at 550 nm (Figure 1C), consistent with the presence of mitochondrial cytochromes [33].

Although the reduced-minus-oxidized spectra of the P3 sample from wild-type HEK-293 cells revealed a small peak, the responsible haem protein was not mitochondrial in origin (Figure 1A) and was unrelated to the Nox protein family, as neither

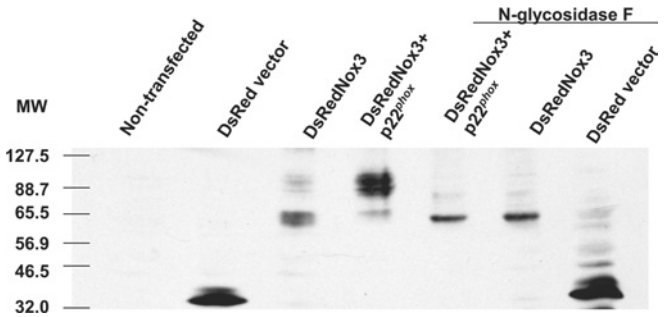

Figure 4 Role of p22^{phox} in the maturation of Nox3

Wild-type HEK-293 cells (untransfected) or HEK-293 cells transfected with DsRed, DsRed–Nox3, or DsRed–Nox3 and p22^{phox} were lysed and treated with buffer or with PNGase F before separation by SDS/PAGE and probing with an anti-DsRed antibody. The relative amounts of the high-molecular-mass Nox3-related proteins recognized by the anti-DsRed antibody were increased by the co-expression of p22^{phox}. These same proteins were susceptible to digestion with PNGase F, indicating that they represented glycosylated forms of Nox3. MW, molecular mass markers in kDa.

wild-type HEK-293 cells nor those transfected with NoxA1 and NoxO1 alone generate superoxide anion [12]. Furthermore, PCR for Nox5 or the related dual oxidases (Duox) failed to recover amplicons from wild-type HEK-293 cells (results not shown). Thus the spectrum detected in P3 of the wild-type HEK-293 cells probably reflected the presence of an uncharacterized endogenous *b*-type cytochrome, such as cytochrome b_5 [34], unrelated to Nox proteins. With the exception of flavocytochrome b_{558}, and perhaps some early measurements of Nox-related plant plasma membrane b_{558} cytochromes [35], this is the first spectroscopic analysis of a Nox protein family member and suggests that the other most closely related members of the family, namely Nox1 and Nox4, would likewise share this structural feature.

To assess the requirement for haem acquisition in Nox3 function, we examined the superoxide-generating capacity of Nox3O1A1 cells cultured in the presence of SA [succinyl acetone (4,6-dioxoheptanoic acid)], an inhibitor of 5-aminolevulinic dehydratase in the haem biosynthetic pathway [36]. When gp91^{phox}–p22^{phox}-expressing cells are cultured in SA, haem incorporation is inhibited and gp91^{phox} maturation is blocked, with secondary impairment of agonist-dependent superoxide generation [10]. SA treatment of the Nox3O1A1 cells did not affect cell viability, as judged by Trypan Blue exclusion (results not shown), but significantly inhibited the constitutive production of superoxide anion. In the presence of 83 μM SA for 48 h, superoxide production by Nox3O1A1 cells was reduced to 16.7 ± 9 % of control ($n = 3$), demonstrating that Nox3 function depended on haem acquisition.

Nox3 is glycosylated and associates with p22^{phox}

Although the primary amino acid sequence of Nox3 has been predicted from its cDNA, recognition of specific features of the protein has been limited by the lack of selective immunochemical probes [37]. To examine the primary translation product for Nox3, its cDNA was used to prime TNT *in vitro* using [^{35}S]methionine in a rabbit reticulocyte lysate system. Using the same vector with gp91^{phox} as a positive control, translation was examined in the absence or presence of added canine microsomal membrane, thereby providing the cellular machinery required for co-translational glycosylation. gp91^{phox} underwent co-translational glycosylation with an attendant increase in molecular mass of $\sim$5 kDa (Supplementary Figure 1S at http://www.BiochemJ.org/bj/403/bj4030097add.htm), consistent with our previous studies demonstrating co-translational N-linked glycosylation of gp91^{phox} [8]. Similarly, the *in vitro* translation of Nox3 cDNA produced an $\sim$50 kDa primary translation product that shifted to $\sim$53 kDa in the presence of canine microsomes (Supplementary Figure 1S). Thus Nox3 underwent co-translational N-linked glycosylation when expressed *in vitro*. The functional significance of the extensive glycosylation of gp91^{phox} is not known, as it is not required for heterodimer formation with p22^{phox} or for enzymatic activity [10]. Whereas gp91^{phox} undergoes glycosylation at three

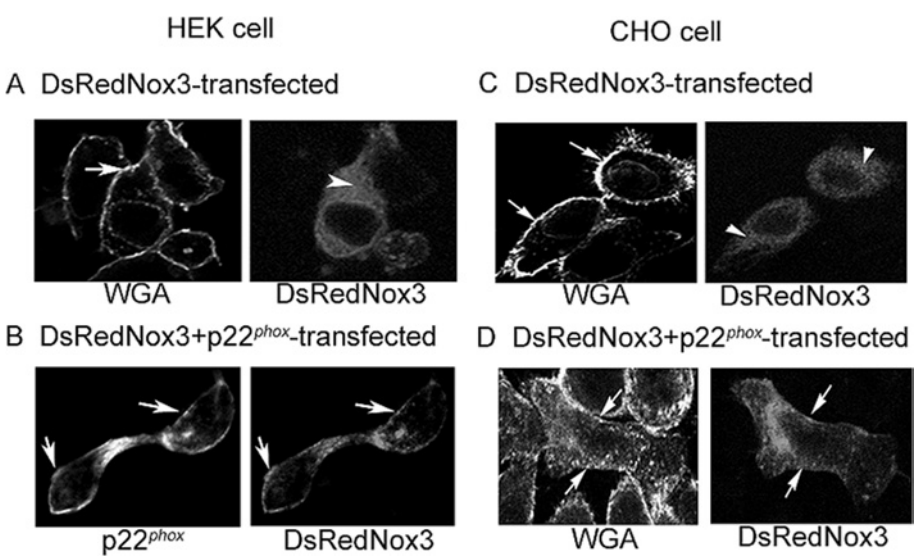

Figure 5 Localization of DsRed–Nox3

HEK-293 cells (**A**, **B**) or CHO cells (**C**, **D**) were examined 3 days after transfection with DsRed–Nox3 alone (**A**, **C**) or in combination with p22^{phox} (**B**, **D**). Where indicated, plasma membranes were detected using Alexa Fluor® 488–WGA and p22^{phox} was detected using anti-p22^{phox} antibody and the Tyramine Signal Amplification kit (**B**). DsRed accumulated in the cytoplasm (arrowheads) in wild-type HEK-293 cells (**A**) as did DsRed–Nox3 in wild-type CHO cells (**C**). However, DsRed–Nox3 and p22^{phox} localized at the plasma membrane (arrows) in HEK-293 cells co-transfected with DsRed–Nox3 and p22^{phox} (**B**) and in p22^{phox} CHO cells (**D**).

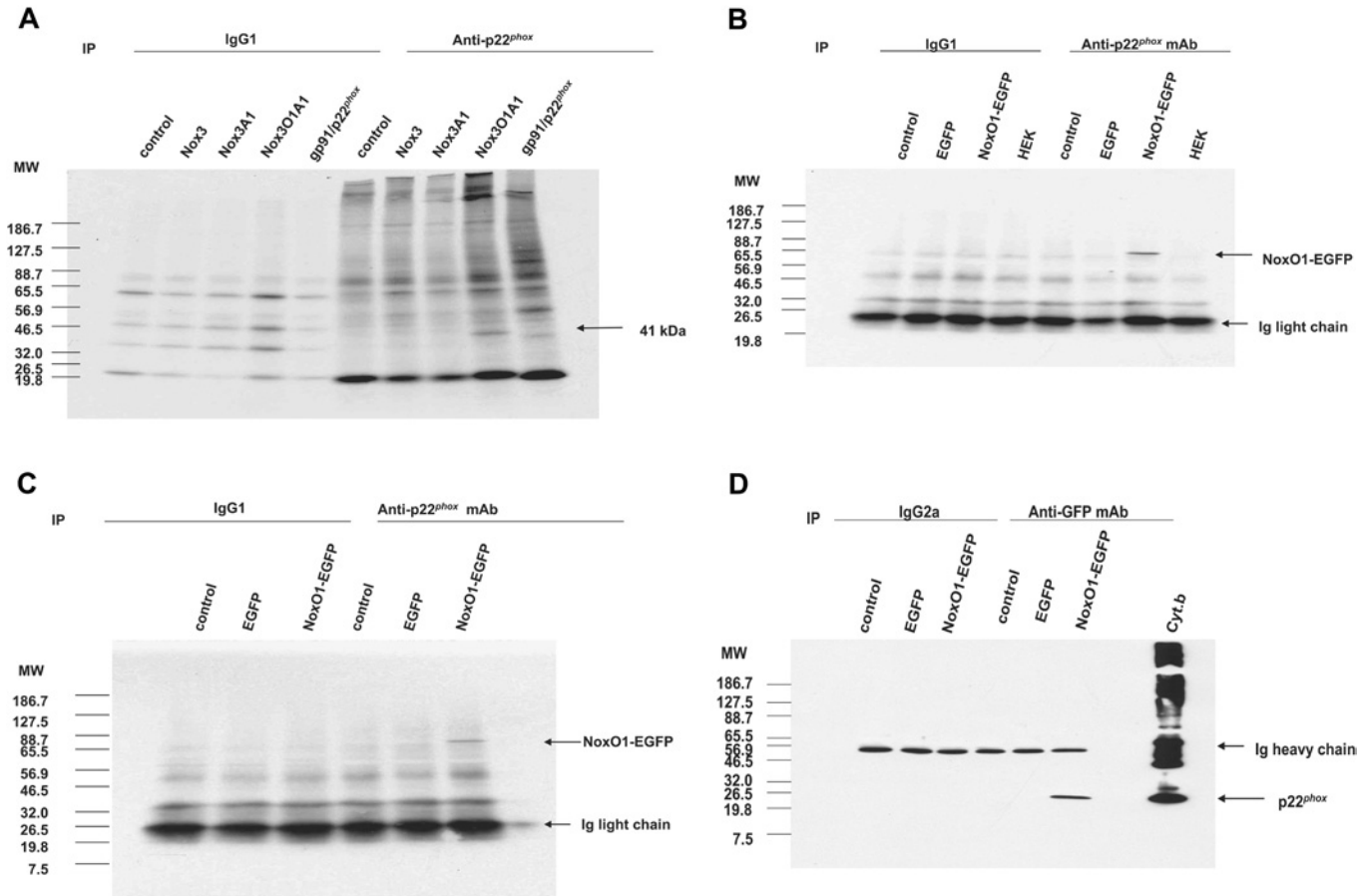

Figure 6 A 41 kDa protein in Nox3O1A1-transfected HEK-293 cells co-immunoprecipitated with p22^{phox}

(**A**) Nox3-transfected HEK-293 cells, Nox3- and NoxA1-transfected HEK-293 cells, Nox3-, NoxA1- and NoxO1-transfected HEK-293 cells, or gp91/p22^{phox}-transfected or untransfected HEK-293 cells were pulse-labelled with [^{35}S]methionine for 1 h. p22^{phox} (CS9) and control (IgG1) immunoprecipitates were resolved by SDS/PAGE. CS9 immunoprecipitated p22^{phox} from all cell lysates and a 41 kDa protein only from Nox3O1A1 transfectants. Nox3A1 HEK-293 cells (**B**, **D**) or wild-type cells (**C**) were transfected with EGFP or NoxO1–EGFP. Cells were solubilized 48 h after transfection, and lysates were immunoprecipitated using CS9 or an isotype control (IgG1) (**B**, **C**), or an anti-GFP antibody or its isotype control (IgG2a) (**D**). The immunoprecipitated proteins were resolved by SDS/PAGE and probed with antibodies against GFP (**B**, **C**) or against p22^{phox} (**D**). CS9 specifically immunoprecipitated only from cells transfected with NoxO1–EGFP, a protein of ~68 kDa that was recognized by anti-GFP antibody (**B**, **C**). The same protein was immunoprecipitated by GFP antibodies and recognized by antibody against p22^{phox} (**D**). NoxO1–GFP and p22^{phox} co-immunoprecipitated independent of the presence of Nox3. IP, immunoprecipitaion; MW, molecular mass markers in kDa.

asparagine residues [38], Nox3 appeared to be modified in the *in vitro* TNT system at only one or two residues, based on the relative shift of ~2.6 kDa for each oligosaccharide unit added in the ER [39]. With better immunochemical probes it will be possible to assess the extent and functional consequences of Nox3 glycosylation in transfected cell lines.

In cultured myeloid cells, heterodimer formation is a prerequisite for stable expression of gp91^{phox}; in the absence of p22^{phox}, precursors of gp91^{phox} fail to reach the plasma membrane and are retained and degraded in the ER [40,41]. Furthermore, patients with the genetic absence of normal gp91^{phox} or p22^{phox} lack both subunits from their affected phagocytes [42], supporting the concept that the free subunits are unstable. In non-myeloid cells, gp91^{phox} free of p22^{phox} can escape the ER and reach the plasma membrane [9], but the process is very inefficient. To determine if Nox3 and p22^{phox} formed functional heterodimers, we assessed the impact of p22^{phox} expression on Nox3. HEK-293 cells express low levels of endogenous p22^{phox} but heterologous expression of gp91^{phox} alone (Figure 2A) or Nox3O1A1 (Figure 2B) increased the steady-state levels of p22^{phox}, suggesting that Nox3 and gp91^{phox} each increased the amount of p22^{phox} protein in HEK-293 cells. Transfection of gp91^{phox} into HEK-293 cells did not increase endogenous p22^{phox} mRNA (results not shown), suggesting that the observed increase in p22^{phox} protein reflected a post-transcriptional event, such as the formation of heterodimers of Nox3–p22^{phox} or gp91^{phox}–p22^{phox} respectively.

We reasoned that heterodimer formation, if truly a prerequisite for egress from the ER and transport to the plasma membrane, should be reflected in increased oxidase function. To determine if p22^{phox} contributed to the function of Nox3, we used a p22^{phox}-specific synthetic siRNA to reduce endogenous p22^{phox} in HEK-293 transfectants. siRNA treatment of the Nox3O1A1-transfected cells decreased p22^{phox} protein to 12 % of the amount in cells treated with scramble control siRNA (Figure 3A). siRNA-mediated depletion of p22^{phox} significantly decreased superoxide anion production in comparison with Nox3O1A1 transfectants that were untreated or exposed to the scramble control construct, 40.3 and 48.5 % respectively (Figure 3B), demonstrating that p22^{phox} expression contributed to the enzymatic activity of Nox3. Taken together, the observations that Nox3 expression increased p22^{phox} levels (Figure 2B) and decreased p22^{phox} protein compromised Nox3-dependent extracellular superoxide production (Figure 3B), suggest that the association of Nox3 and p22^{phox} into heterodimers was necessary for optimal function.

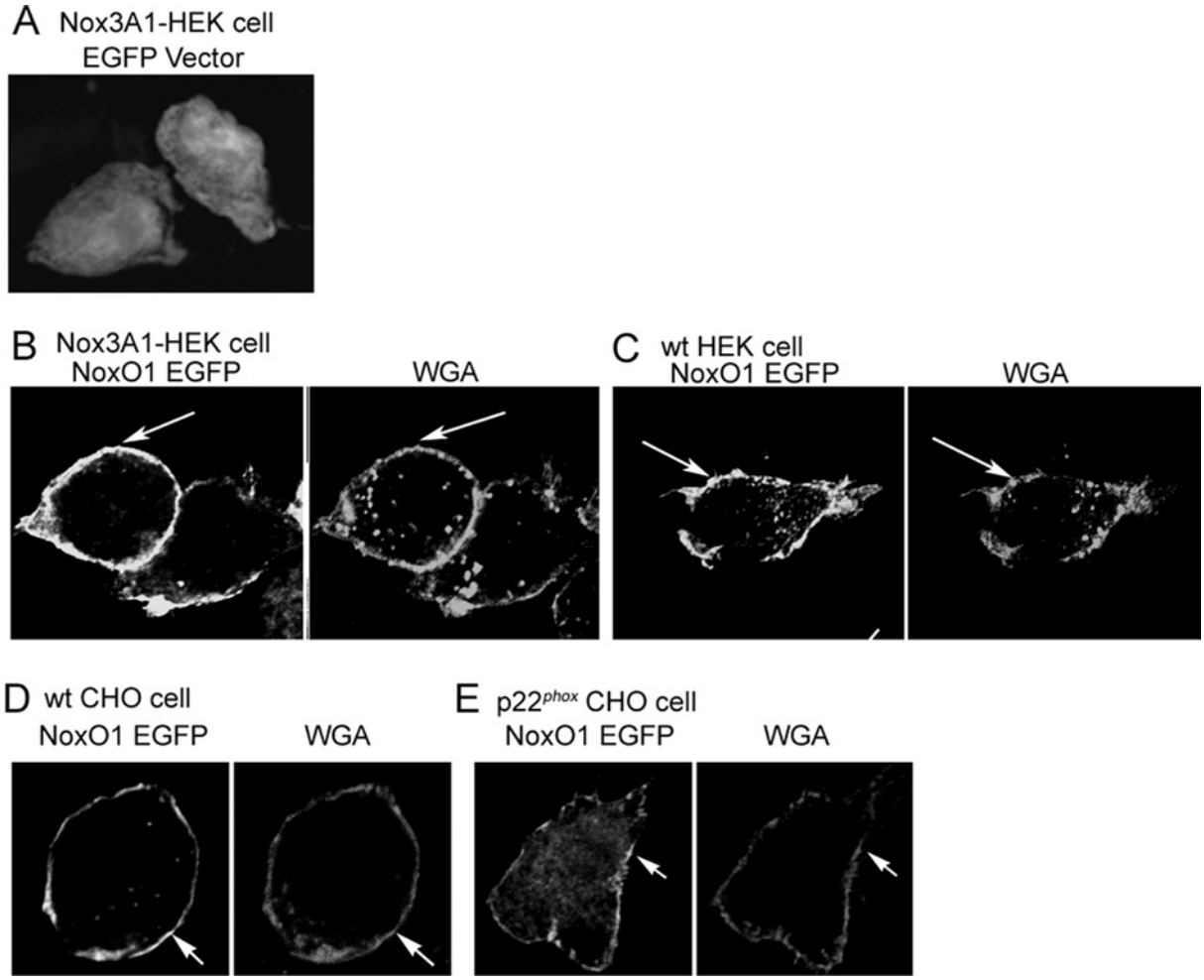

Figure 7 NoxO1 localized in the plasma membrane in the presence or absence of Nox3 and p22^{phox}

Nox3A1 HEK-293 cells (**A**, **B**) wild-type HEK-293 cells (**C**), wild-type CHO cells (**D**) or p22^{phox} CHO cells (**E**) were transfected with EGFP vector (**A**) or with NoxO1–EGFP (**B**–**E**). Two days after transfection, fixed cells were stained with Alexa Fluor® 594-conjugated WGA. Whereas EGFP accumulated in the cytoplasm (**A**), NoxO1 localized at the plasma membrane (arrows) in HEK-293 cells (**B**, **C**) or CHO cells (**D**, **E**), co-localizing with WGA and independent of the presence of Nox3 or p22^{phox}.

p22^{phox} and the cellular fate of Nox3

The data shown in Figure 3(B) suggest that heterodimer formation may be a prerequisite for Nox structural maturation and trafficking to the plasma membrane. To address this issue, we examined the cellular location of DsRed–Nox3 using confocal microscopy and assessed the glycosylation state of Nox3. Because fusion proteins of Nox family members often lack functional activity [43], we first confirmed that HEK-293 cells transfected with the DsRed-fused Nox3, NoxO1pcDNA, and NoxA1pcDNA produced superoxide anion [7.84 nmol $\cdot$ (10^6 cells)$^{-1}$ $\cdot$ h^{-1} after transfection with 0.4 μg of each plasmid]. Not only was the DsRed-fused Nox3 protein functional, but transfection with DsRed–Nox3 also increased the level of endogenous p22^{phox} (results not shown), suggesting that DsRed–Nox3 interacted with endogenous p22^{phox}, as did Nox3 in stable Nox3O1A1 transfectants.

We examined first the effect of p22^{phox} expression on the glycosylation state of Nox3 in HEK-293 transfectants. The antibody against DsRed recognized several proteins in DsRed–Nox3 transfectants that were not present in wild-type HEK-293 cells or DsRed vector transfectants (Figure 4). Co-transfection of p22^{phox} into DsRed–Nox3-expressing HEK-293 cells increased the amount of higher molecular mass proteins ($\sim$100 kDa) recognized by anti-DsRed antibody. Simultaneously there was a decrease in the lower molecular mass species, consistent with the conversion of intermediate Nox3 species into more mature forms by glycosylation. The 65 kDa species, which is likely to be a degradation product of DsRed–Nox3, was also decreased in the presence of p22^{phox}, consistent with the ability of p22^{phox} co-expression to rescue Nox3 from degradation in the ER. We confirmed that the increased appearance of higher molecular mass proteins was the result of glycosylation by assessing their susceptibility to PNGase F digestion. Taken together, these data suggest that p22^{phox} served important roles both in the maturation and stability of Nox3. Using CHO cells, we also examined the glycosylation state of DsRed–Nox3 in the absence of p22^{phox}, since wild-type CHO cells lack endogenous p22^{phox} mRNA or protein [45]. Whereas wild-type cells transfected with DsRed–Nox3 lacked high-molecular-mass species, the lysate from the p22^{phox} CHO cells expressed several high-molecular-mass proteins recognized by anti-DsRed antibody that were consistent with glycosylated Nox3, suggesting that p22^{phox} was necessary for Nox3 maturation (results not shown).

We reasoned that the structural maturation of DsRed–Nox3 would parallel its targeting to the plasma membrane, and to test this prediction we examined the subcellular distribution of the

fusion protein in both HEK-293 and CHO-K1 transfectants. DsRed alone was diffusely distributed in the cytosol of HEK-293 transfectants (results not shown) and DsRed–Nox3 was distributed primarily in the cytosol of wild-type HEK-293 cells with limited staining of plasma membrane or Golgi, as judged by lack of co-localization with WGA (Figure 5A). Co-transfection of p22^{phox} with DsRed–Nox3 in HEK-293 cells increased the amount of DsRed–Nox3 at the plasma membrane where it co-localized with p22^{phox} (Figure 5B). In addition, the percentage of cells demonstrating plasma membrane DsRed–Nox3 was significantly increased by co-transfection of p22^{phox}: 78.5 ± 12.7 % versus 25.1 ± 12.6 % respectively. These data suggest that p22^{phox} enhanced membrane targeting of Nox3 in HEK-293 cells. The limited membrane localization of DsRed–Nox3 in wild-type HEK-293 cells probably reflected the contribution of endogenous p22^{phox}. To more rigorously assign the membrane targeting of Nox3 to p22^{phox}, we also examined the localization of DsRed–Nox3 in CHO-K1 cells, which lack endogenous p22^{phox}. Whereas DsRed–Nox3 was expressed diffusely in cytosol and did not localize in plasma membrane in wild-type CHO cells (Figure 5C), small amounts of DsRed–Nox3 localized at the plasma membrane in CHO cells stably transfected with p22^{phox} (Figure 5D) and co-localized with WGA. These data suggest that p22^{phox} associated with Nox3 and that the interaction was required for successful targeting of Nox3 to the plasma membrane. Taken together, the biochemical and confocal microscopy data indicate that p22^{phox} promoted plasma membrane targeting of Nox3, possibly via its effects on both protein maturation and stability. Our findings complement and extend recently published work on the organization of the Nox3-dependent oxidase [46–48] and further suggest that heterodimer formation is likely to be an essential prerequisite for Nox3 function.

Role of NoxO1 in p22^{phox} and Nox3 interactions

Just as the phagocyte Nox has cytosolic components essential for flavocytochrome b_{558} function [1,2,4,5], murine Nox3 requires NoxO1 and NoxA1 for optimal activity [12]. Considering potential interactions that NoxO1 might mediate with p22^{phox} and with Nox3, we reasoned that p22^{phox} could influence enzymatic activity directly by its association with Nox3, indirectly via interactions with NoxO1, or both. To identify the proteins that interacted with endogenous p22^{phox}, wild-type HEK-293 cells or cells stably transfected with Nox3, Nox3A1 or Nox3O1A1 were pulse-labelled with [^{35}S]methionine and immunoprecipitated with CS9, a murine anti-p22^{phox} antibody [49]. Although these conditions did not completely solubilize Nox3 [37], a 41 kDa protein co-precipitated with endogenous p22^{phox} only in the cells expressing NoxO1, a protein with a predicted molecular mass of 41 kDa (Figure 6A).

Since antibodies that immunoprecipitate murine NoxO1 are not available, we transfected EGFP–NoxO1 into the stable Nox3A1-transfected HEK-293 cells or HEK-293 wild-type cells to examine interactions with p22^{phox}. A protein of $\sim$68 kDa, the anticipated size of the EGFP–NoxO1 fusion protein, co-immunoprecipitated with endogenous p22^{phox} in both Nox3A1-transfected cells (Figure 6B) and wild-type HEK-293 cells (Figure 6C). Furthermore, when GFP immunoprecipitates were probed with anti-p22^{phox} antibody, EGFP–NoxO1 co-immunoprecipitated with p22^{phox} in Nox3O1A1 (Figure 6D) or wild-type HEK-293 cells (results not shown). Thus NoxO1 and p22^{phox} were linked in a stable complex that could be recovered by immunoprecipitation with antibodies directed against either protein. Furthermore, p22^{phox} complexed with NoxO1 in the absence or presence of Nox3. Consistent with the interpretation that NoxO1–p22^{phox} interactions were independent of Nox3, the levels of endogenous p22^{phox} increased when NoxO1–EGFP was expressed in either Nox3A1-transfected or wild-type HEK-293 cells (results not shown).

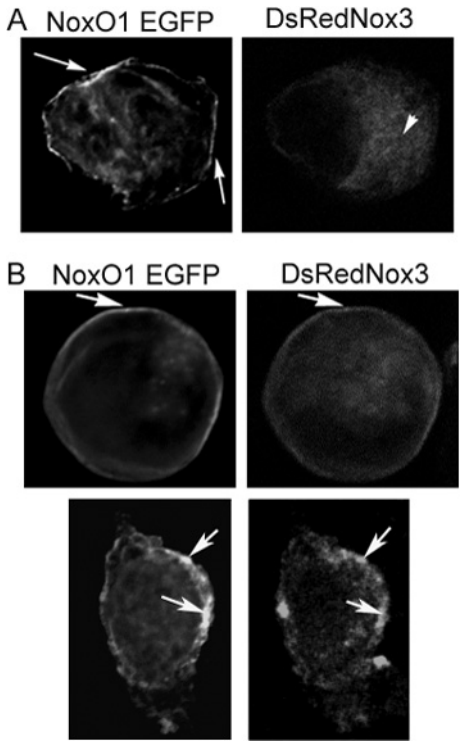

Figure 8 NoxO1 and Nox3 in the presence of p22^{phox}

Wild-type (**A**) or p22^{phox} (**B**) CHO cells were co-transfected with NoxO1–EGFP and DsRed–Nox3 and were analysed by confocal microscopy on day 3. NoxO1 and Nox3 co-localized at the plasma membrane only in the presence of p22^{phox} (arrows), whereas Nox3 accumulated in the cytoplasm in wild-type CHO cells (arrowhead).

p22^{phox} and NoxO1 localization at the plasma membrane

Since p22^{phox} and NoxO1 associated independent of Nox3, we reasoned that p22^{phox} might stabilize NoxO1 at the plasma membrane, much in the way it had enhanced surface expression of Nox3 (Figure 5). Alternatively NoxO1 might associate with the plasma membrane via its phosphatidylinositol-binding PX domain (Phox homology domain) [43,44] and independent of p22^{phox}. To determine which of the two possibilities applied, we used confocal microscopy to assess the subcellular localization of EGFP–NoxO1 (Figure 7). EGFP–NoxO1 was functional in Nox3A1 HEK-293 transfectants (results not shown) and thus correctly integrated into the plasma membrane in the presence of p22^{phox} and co-localized there with WGA. EGFP vector alone, used as a negative control, was distributed diffusely in the cytoplasm (Figure 7A).

In HEK-293 cells, either transfectants expressing Nox3 and NoxA1 (Figure 7B) or wild-type (Figure 7C), EGFP–NoxO1 was detected at the plasma membrane where it co-localized with WGA. EGFP vector alone, on the other hand, was not at the cell surface (Figure 7A). Thus NoxO1 was targeted to the membrane independent of Nox3 or NoxA1. However, the relative contributions of the endogenous p22^{phox} in HEK-293 cells and of the PX domain of NoxO1 to the fate of NoxO1 were not resolved. To focus specifically on the contribution of p22^{phox}, we assessed the fate of EGFP–NoxO1 in wild-type (Figure 7D) and p22^{phox} CHO cells (Figure 7E). As in HEK-293 transfectants, EGFP–NoxO1 was targeted to the plasma membrane in CHO-K1 cells

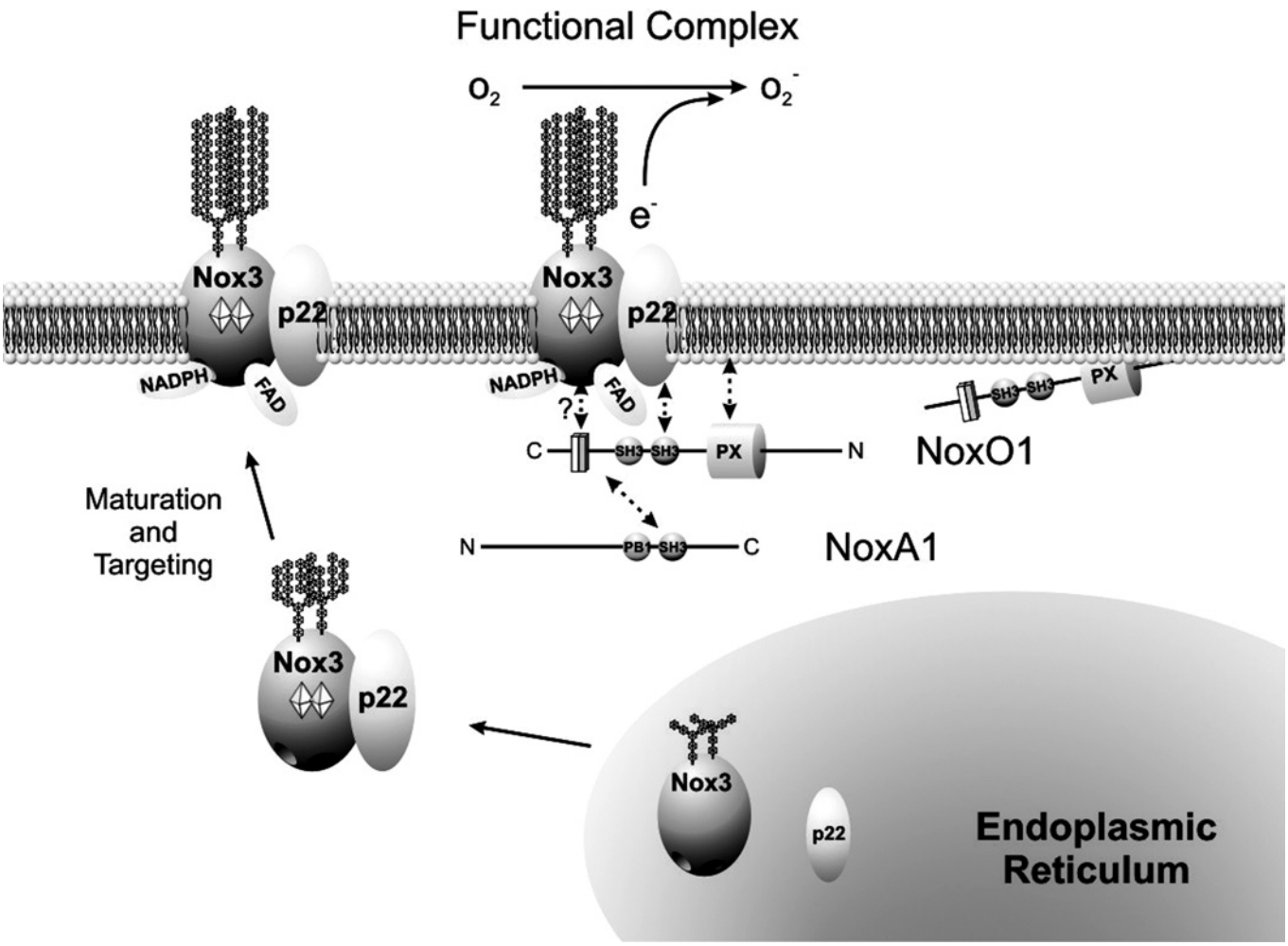

Figure 9 Contributions of p22^{phox} to the maturation and membrane targeting of Nox3

Nox3 and p22^{phox} are independently synthesized in the ER, with Nox3 undergoing co-translational N-linked glycosylation (branched structures). Association of p22^{phox} with Nox3 is a prerequisite for efficient egress from the ER, subsequent oligosaccharide maturation in the Golgi, and targeting to the cell surface. However, Nox3–p22^{phox} heterodimers lack oxidase activity in the absence of NoxO1 and NoxA1. Similarly, NoxO1 associates with the plasma membrane independent of Nox3, but lacks intrinsic electron transferase activity. Superoxide anion production by Nox3–p22^{phox} heterodimer requires its co-localization with NoxO1 at the plasma membrane and recruitment of NoxA1.

in the absence (Figure 7D) or presence (Figure 7E) of p22^{phox} and co-localized with WGA (Figures 7D and 7E). Taken together, these data indicate that although p22^{phox} associated with NoxO1, NoxO1 associated with the plasma membrane independent of p22^{phox}, most likely via its PX domain. The PX domain of NoxO1 was previously demonstrated to bind selectively to monophosphorylated phosphoinositols (PtdIns), specifically PtdIns(3)*P*, PtdIns(4)*P*, and PtdIns(5)*P*, as well as PtdIns(3,5)P_2 [43,44]. These phospholipids are present in resting cells and thus are likely to support constitutive membrane association and activity in the absence of agonists.

Integration of the functional Nox3 complex

NoxO1 is essential for the full activity of Nox3 and presumably this reflects the existence of a ternary complex that supports the ability of NoxA1 to initiate electron transfer. To test the hypothesis that p22^{phox} was the essential link in a ternary complex also containing Nox3 and NoxO1, we used confocal microscopy to examine the subcellular distribution of EGFP–NoxO1 and DsRed–Nox3 in wild-type or p22^{phox} CHO cells. In wild-type CHO cells, NoxO1 and Nox3 failed to co-localize, as NoxO1 successfully reached the plasma membrane and DsRed–Nox3 remained in the cytoplasm (Figure 8A). However, when NoxO1–EGFP and DsRed–Nox3 were co-transfected into p22^{phox}-CHO cells, a subfraction of NoxO1 and Nox3 was targeted to the plasma membrane (Figure 8B), demonstrating that p22^{phox} was required for Nox3 to reach the plasma membrane regardless of the presence of NoxO1. NoxO1–EGFP and DsRed–Nox3 co-localization was enhanced by co-transfection of p22^{phox} in HEK-293 cells as well (results not shown). Taken together, these findings suggest that p22^{phox} contributed to the enzymatic activity of Nox3, at least in part, by promoting its targeting to the cell surface.

Taken together, these data indicate that Nox3, p22^{phox} and NoxO1 interact at the membrane as a ternary complex. In fact, there are several independent interactions among these three proteins at the plasma membrane. NoxO1 co-immunoprecipitated with p22^{phox} in the absence or presence of Nox3, demonstrating that p22^{phox} associated with NoxO1 in a stable fashion. Previous demonstration that a GST (glutathione S-transferase) fusion protein containing the SH3 (Src homology 3) domains of NoxO1 recovers p22^{phox} in pull-down experiments [46] implicates the SH3 domains of NoxO1 in mediating its association with p22^{phox}. Furthermore, p22^{phox} with a mutation (P156H) in its proline-rich

region fails to associate with NoxO1 [47]. Collectively, these data demonstrate that assembly depends on the interaction between the SH3 domains of NoxO1 and the proline-rich region of p22^{phox} (Figure 9). However, NoxO1 localized to the plasma membrane in CHO cells, which lack endogenous p22^{phox} or Nox3, an event most likely mediated by interactions of the PX domain of NoxO1 with membrane phospholipids [43,44]. Consistent with this interpretation, our confocal microscopy data always detected NoxO1 at the plasma membrane, demonstrating that the constitutive targeting of NoxO1 was independent of the presence of the other Nox components. Unlike NoxO1, Nox3 required co-expression of p22^{phox} to reach the plasma membrane and vice versa [46]. Expressed in HEK-293 cells and targeted to the plasma membrane, NoxO1 alone fails to support superoxide production even in the presence of endogenous p22^{phox} [13]. Heterodimer formation was necessary for either Nox3 or p22^{phox} to reach the plasma membrane, where oxidant production is low unless NoxO1 and NoxA1 are co-expressed [12]. Thus, although constitutively associated with the plasma membrane, NoxO1 appears to have functional consequences only when co-localized in membrane domains containing Nox3 and p22^{phox}.

Collectively, our results and recently published studies [46–48] implicate p22^{phox} as an essential factor in the successful development of a functional Nox3 complex at several important steps (Figure 9). The association of p22^{phox} with Nox3 in the ER stabilizes each subunit within a heterodimer that acquires haem (Figure 9, diamonds) and advances from ER to Golgi, where high-mannose oligosaccharides are converted into more complex structures (Figure 9, chains). Heterodimer formation is a prerequisite for the structural maturation of Nox3 and its targeting to the cell surface. NoxO1 associates at the cell surface even in the absence of Nox3 by virtue of its PX domain [43,44] and associates with p22^{phox} even in the absence of Nox3 (Figure 7), perhaps via interactions between its SH3 domain and the proline-rich motif in p22^{phox} [47] (Figure 9). However, in the absence of p22^{phox}, Nox3 fails to reach the cell surface and the capacity for superoxide generation is ablated. Thus p22^{phox} is essential both for proper maturation and targeting of Nox3 to the cell surface and for optimal orientation of NoxO1 in proximity to the Nox3–p22^{phox} heterodimer at the membrane to yield a functional complex. In this way p22^{phox} is essential in the functional organization of Nox3 at the cell surface. These data extend our understanding of the structural features and organization of the functional Nox3 complex and the central role of p22^{phox}.

This research was supported by grants RO1 AI26711 (A.J.J.), HL45635 (M.C.D.), and AI34879 and HL53592 (W.M.N.) from the National Institutes of Health, United States Public Health Service. We thank Melissa Goedken, Kevin Leidal, Angela Nelson, Sally McCormick and Jamie Schlomann for technical support and assistance and Tom Nelson for his creative input on Figure 9.

REFERENCES

1 Babior, B. M., Lambeth, J. D. and Nauseef, W. (2002) The neutrophil NADPH oxidase. Arch. Biochem. Biophys. **397**, 342–344
2 Quinn, M. T. and Gauss, K. A. (2004) Structure and regulation of the neutrophil respiratory burst oxidase: comparison with nonphagocyte oxidases. J. Leukoc. Biol. **76**, 760–781
3 Cross, A. R. and Segal, A. W. (2004) The NADPH oxidase of professional phagocytes-prototype of the NOX electron transport chain systems. Biochim. Biophys. Acta **1657**, 1–22
4 Nauseef, W. M. (2004) Assembly of the phagocyte NADPH oxidase. Histochem. Cell Biol. **122**, 277–291
5 Babior, B. M. (1999) NADPH oxidase: an update. Blood **93**, 1464–1476
6 Heyworth, P. G., Cross, A. R. and Curnutte, J. T. (2003) Chronic granulomatous disease. Curr. Opin. Immunol. **15**, 578–584
7 Nauseef, W. M. and Clark, R. A. (2005) Granulocytic phagocytes. In Principles and Practice of Infectious Diseases (Mandell, G. L., Bennett, J. E. and Dolin, R., eds.), pp. 93–117, Churchill-Livingstone, Philadelphia, NJ
8 Yu, L., DeLeo, F. R., Biberstine-Kinkade, K. J., Renee, J., Nauseef, W. M. and Dinauer, M. C. (1999) Biosynthesis of flavocytochrome b_{558}. J. Biol. Chem. **274**, 4364–4369
9 Yu, L. and Dinauer, M. C. (1997) Biosynthesis of the phagocyte NADPH oxidase cytochrome b_{558}. J. Biol. Chem. **272**, 27288–27294
10 DeLeo, F. R., Burritt, J. B., Yu, L., Jesaitis, A. J., Dinauer, M. C. and Nauseef, W. M. (2000) Processing and maturation of flavocytochrome b_{558} includes incorporation of heme as a prerequisite for heterodimer assembly. J. Biol. Chem. **275**, 13986–13993
11 Cheng, G., Cao, Z., Xu, X., Van Meir, E. and Lambeth, J. (2001) Homologs of gp91phox: cloning and tissue expression of Nox3, Nox4, and Nox5. Gene **269**, 131–140
12 Banfi, B., Malgrange, B., Knisz, J., Steger, K., Dubois-Dauphin, M. and Krause, K.-H. (2004) NOX3, a superoxide-generating NADPH oxidase of the inner ear. J. Biol. Chem. **279**, 46065–46072
13 Bánfi, B., Clark, R. A., Steger, K. and Krause, K.-H. (2003) Two novel proteins activate superoxide generation by the NADPH oxidase NOX1. J. Biol. Chem. **278**, 3510–3513
14 Takeya, R., Ueno, N., Kami, K., Taura, M., Kohjima, M., Izaki, T., Nunoi, H. and Sumimoto, H. (2003) Novel human homologues of p47^{phox} and p67^{phox} participate in activation of superoxide-production NADPH oxidases. J. Biol. Chem. **278**, 25234–25246
15 Cheng, G., Ritsick, D. and Lambeth, J. D. (2004) Nox3 regulation by NOXO1, p47^{phox}, and p67^{phox}. J. Biol. Chem. **279**, 34250–34255
16 Kiss, P. J., Knisz, J., Zhang, Y., Baltrusaitis, J., Sigmund, C. D., Thalmann, R., Smith, R. J. H., Verpy, E. and Banfi, B. (2006) Inactivation of NADPH oxidase organizer 1 results in severe imbalance. Curr. Biol. **16**, 208–213
17 Paffenholz, R., Bergstrom, R. A., Pasutto, F., Wabnitz, P., Munroe, R. J., Jagla, W., Heinzmann, Y., Marquardt, A., Bareiss, A., Laufs, J. et al. (2004) Vestibular defects in head-tilt mice result from mutations in nox3, encoding an NADPH oxidase. Genes Dev. **18**, 486–491
18 Nakamura, M., Murakami, M., Koga, T., Tanaka, Y. and Minakami, S. (1987) Monoclonal antibody 7D5 raised to cytochrome b_{558} of human neutrophils: immunocytochemical detection of the antigen in peripheral phagocytes of normal subjects, patients with chronic granulomatous disease, and their carrier mothers. Blood **69**, 1404–1408
19 Emmendorffer, A., Nakamura, M., Rothe, G., Spiekermann, K., Lohmann-Matthes, M. L. and Roesler, J. (1994) Evaluation of flow cytometric methods for diagnosis of chronic granulomatous disease variants under routine laboratory conditions. Cytometry **18**, 147–155
20 Burritt, J. B., DeLeo, F. R., McDonald, C. L., Prigge, J. R., Dinauer, M. C., Nakamura, M., Nauseef, W. M. and Jesaitis, A. J. (2001) Phage display epitope mapping of human neutrophil flavocytochrome b_{558}. Identification of two juxtaposed extracellular domains. J. Biol. Chem. **276**, 2053–2061
21 Burritt, J. B., Quinn, M. T., Jutila, M. A., Bond, C. W. and Jesaitis, A. J. (1995) Topological mapping of neutrophil cytochrome b epitopes with phage-display libraries. J. Biol. Chem. **270**, 16974–16980
22 Burritt, J. B., Busse, S. C., Gizachew, D., Siemsen, D. W., Quinn, M. T., Bond, C. W., Dratz, E. A. and Jesaitis, A. J. (1998) Antibody imprint of a membrane protein surface. J. Biol. Chem. **273**, 24847–24852
23 Parkos, C. A., Allen, R. A., Cochrane, C. G. and Jesaitis, A. J. (1987) Purified cytochrome b from human granulocyte plasma membrane is comprised of two polypeptides with relative molecular weights of 91000 and 22000. J. Clin. Invest. **80**, 732–742
24 Cross, A. R., Higson, F. K. and Jones, O. T. G. (1982) The enzymic reduction and kinetics of oxidation of cytochrome *b* of neutrophils. Biochem. J. **204**, 479–485
25 Nauseef, W. M., Metcalf, J. A. and Root, R. K. (1983) Role of myeloperoxidase in the respiratory burst of human neutrophils. Blood **61**, 483–491
26 Babior, B. M., Kipnes, R. S. and Curnutte, J. T. (1973) Biological defence mechanisms. The production by leukocytes of superoxide, a potential bactericidal agent. J. Clin. Invest. **52**, 741–744
27 Wood, J. G., Byrd, F. I. and Gurd, J. W. (1981) Lectin cytochemistry of carbohydrates on cell membranes of rat cerebellum. J. Neurocytol. **10**, 149–159
28 Winqvist, L., Eriksson, L. C. and Dallner, G. (1979) Interaction of lectins with proteins of the endoplasmic reticulum and Golgi system of rat liver. J. Cell Sci. **39**, 101–116
29 Yu, L., Quinn, M. T., Cross, A. R. and Dinauer, M. C. (1998) Gp91^{phox} is the heme binding subunit of the superoxide-generating NADPH oxidase. Proc. Natl. Acad. Sci. U.S.A. **95**, 7993–7998
30 Biberstine-Kinkade, K. J., DeLeo, F. R., Epstein, R. I., LeRoy, B. A., Nauseef, W. M. and Dinauer, M. C. (2001) Heme-ligating histidines in flavocytochrome b_{558}. J. Biol. Chem. **276**, 31105–31112
31 Harper, A. M., Dunne, M. J. and Segal, A. W. (1984) Purification of cytochrome *b*-245 from human neutrophils. Biochem. J. **219**, 519–527

32 Cross, A. R., Jones, O. T. G., Harper, A. M. and Segal, A. W. (1981) Oxidation-reduction properties of the cytochrome *b* found in the plasma-membrane fraction of human neutrophils. A possible oxidase in the respiratory burst. Biochem. J. **194**, 599–606
33 Choi, S. and Swanson, J. M. (1995) Interaction of cytochrome c with cardiolipin: an infrared spectroscopic study. Biophys. Chem. **54**, 271–278
34 Aoyama, T., Nagata, K., Yamazoe, Y., Kato, R., Matsunaga, E., Gelboin, H. V. and Gonzalez, F. J. (1990) Cytochrome b_5 potentiation of cytochrome P-450 catalytic activity demonstrated by a vaccinia virus-mediated *in situ* reconstitution system. Proc. Natl. Acad. Sci. U.S.A. **87**, 5425–5429
35 Jesaitis, A. J., Heners, P. R. and Hertel, R. (1977) Characterization of a membrane fraction containing a *b*-type cytochrome. Plant Physiol. **59**, 941–947
36 Ebert, P. S., Hess, R. A., Frykholm, B. C. and Tschudy, D. P. (1979) Succinylacetone, a potent inhibitor of heme biosynthesis: effect on cell growth, heme content, and delta-aminolevulinic acid dehydratase activity of malignant murine erythroleukemia cells. Biochem. Biophys. Res. Commun. **88**, 1382–1390
37 Baniulis, D., Nakano, Y., Nauseef, W. M., Banfi, B., Cheng, G., Lambeth, D. J., Burritt, J. B., Taylor, R. M. and Jesaitis, A. J. (2005) Evaluation of two anti-gp91 (phox) antibodies as immunoprobes for Nox family proteins: mAb 54.1 recognizes recombinant full-length Nox2, Nox3 and the C-terminal domains of Nox1-4 and cross-reacts with GRP 58. Biochim. Biophys. Acta **1752**, 186–196
38 Wallach, T. M. and Segal, A. W. (1997) Analysis of glycosylation sites on gp91phox, the flavocytochrome of the NADPH oxidase, by site-directed mutagenesis and translation *in vitro*. Biochem. J. **321**, 583–585
39 Nauseef, W. M. (1987) Posttranslational processing of a human myeloid lysosomal protein, myeloperoxidase. Blood **70**, 1143–1150
40 Porter, C. D., Parkar, M. H., Verhoeven, A. J., Levinsky, R. J., Collins, M. K. and Kinnon, C. (1994) p22phox-deficient chronic granulomatous disease: reconstitution by retrovirus-mediated expression and identification of a biosynthetic intermediate of gp91phox. Blood **84**, 2767–2775

Received 2 June 2006/30 November 2006; accepted 1 December 2006
Published as BJ Immediate Publication 1 December 2006, doi:10.1042/BJ20060819

41 Maly, F. E., Schuerer-Maly, C. C., Quilliam, L., Cochrane, C. G., Newburger, P. E., Curnutte, J. T., Gifford, M. and Dinauer, M. C. (1993) Restitution of superoxide generation in autosomal cytochrome-negative chronic granulomatous disease (A220 CGD)-derived B lymphocyte cell lines by transfection with p22phox cDNA. J. Exp. Med. **178**, 2047–2053
42 Parkos, C. A., Dinauer, M. C., Jesaitis, A. J., Orkin, S. H. and Curnutte, J. T. (1989) Absence of both the 91kD and 22kD subunits of human neutrophil cytochrome b in two genetic forms of chronic granulomatous disease. Blood **73**, 1416–1420
43 Cheng, G. and Lambeth, J. D. (2004) NOXO1, regulation of lipid binding, localization, and activation of Nox1 by the phox homology (PX) domain. J. Biol. Chem. **279**, 4737–4742
44 Ueyama, T., Lekstrom, K., Tsujibe, S., Saito, N. and Leto, T. L. (2007) Subcellular localization and function of alternatively spliced Noxo1 isoforms. Free Radical Biol. Med. **42**, 180–190
45 Biberstine-Kinkade, K. J., Yu, L., Stull, N., LeRoy, B., Bennett, S., Cross, A. and Dinauer, M. C. (2002) Mutagenesis of $p22^{phox}$ histidine 94. J. Biol. Chem. **277**, 30368–30374
46 Ueno, N., Takeya, R., Miyano, K., Kikuchi, H. and Sumimoto, H. (2005) The NADPH oxidase NOX3 constitutively produces superoxide in a $p22^{phox}$-dependent manner: its regulation by oxidase organizers and activators. J. Biol. Chem. **280**, 23328–23339
47 Kawahara, T., Ritsick, D., Cheng, G. and Lambeth, J. D. (2005) Point mutations in the proline-rich region of $p22^{phox}$ are dominant inhibitors of NOX1- and NOX2-dependent reactive oxygen generation. J. Biol. Chem. **280**, 31859–31869
48 Ueyama, T., Geiszt, M. and Leto, T. L. (2006) Involvement of Rac1 in activation of multicomponent Nox1- and Nox3-based NADPH oxidases. Mol. Cell. Biol. **26**, 2160–2174
49 Taylor, R. M., Burritt, J. B., Baniulis, D., Foubert, T. R., Lord, C. I., Dinauer, M. C., Parkos, C. A. and Jesaitis, A. J. (2004) Site-specific inhibitors of NADPH oxidase activity and structural probes of flavocytochrome b: characterization of six monoclonal antibodies to the $p22^{phox}$ subunit. J. Immunol. **173**, 7349–7357